

pH DEPENDENT STRUCTURES OF BOVINE SERUM IN SOLUTION BY SMALL ANGLE NEUTRON SCATTERING

Arum Patriati*, Edy Giri Rachman Putra

Center for Science and Technology of Advanced Materials, BATAN, Building 43 Kawasan PUSPIPTEK Serpong, Banten 15314, Indonesia

Article history

Received

2 June 2020

Received in revised form

23 December 2020

Accepted

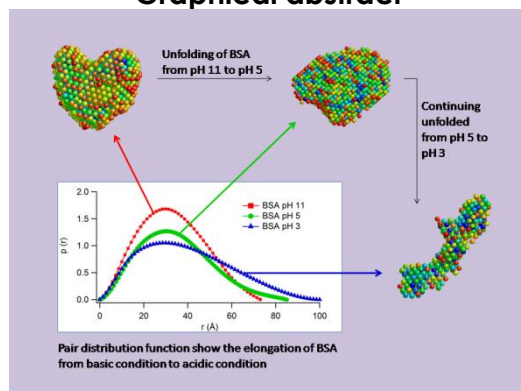
5 January 2021

Published online

23 February 2021

*Corresponding author
arum@batan.go.id

Graphical abstract



Abstract

The pH-dependent structures of the bovine serum albumin (BSA), under physiological conditions that permit enzymatic activity, were investigated by small-angle neutron scattering (SANS). The unfolding behavior of BSA in solution is important to understand the mechanism of protein aggregation due to protein conformational change. The information of protein structure is crucial to design the perfect protein-based drug delivery device. This information will be useful as a complementary data of BSA crystal structure in static state. The structure of BSA in solution was found to be heart shaped, nearly identical to bovine serum albumin crystal structure. The globular heart shaped structure of BSA was still maintained at alkaline pH range of 7 to 11. It underwent partial unfolding at pH 5 and continued to unfold at pH 3. The unfolded-structure of BSA shows that the globular structure started to change into a cylinder-like structure at pH 3 which was clearly shown in Kratky plot. These results were confirmed with ab initio low-resolution shape calculation model analysis using GNOM and DAMMIF in obtaining the three-dimensional protein structure model.

Keywords: BSA, SANS, folding-unfolding, three-dimensional structure, pH dependent

© 2021 Penerbit UTM Press. All rights reserved

1.0 INTRODUCTION

Bovine serum albumin (BSA) is one of abundant proteins in mammalian body. It found in blood stream and milk. It has role in maintaining osmotic pressure of the circulatory system and binding a variety of molecules including toxins. BSA also binds and transports fatty acids. In its physiological condition (pH 7) BSA is a globular protein having a molecular weight of 66 kDa, 583 amino acid residues, and 17 disulfide bridges. Three homologous domains build up BSA, which is called as domain I, II, and III. Each domain is divided into two subdomains (A and B) [1, 2].

BSA has been widely used as drug delivery device because of its non-toxicity, biodegradability, non-immunogenicity, water solubility, availability and its

low cost, because large quantities of it can be readily purified from bovine blood [3]. In order to be used as drug delivery device, BSA has been bound with ligand complex [1] and polymer [4], or complexed with magnetic iron oxide [5].

BSA can undergo conformational change in the variation of pH from expanded (E), to fast (F), normal (N), basic (B) and aged (A) forms. These five isomeric forms of BSA are exist in pH below 2.7 for E form, in $2.7 < \text{pH} < 4.3$ for F form, in $4.3 < \text{pH} < 8$ for N form, in $8 < \text{pH} < 10$ for B form, and in pH more than 10 for A form [6]. As drug delivery device, the conformational stability of BSA at large range of pH becomes important. This information helps to understand the binding drug ability of BSA during synthesis and administration or drug releasing. Furthermore, the

conformational change of BSA as pH change leads to the awareness of the possibility of protein aggregation that may lead to the protein toxicity since several diseases are associated with the protein aggregation like Alzheimer's disease [7] and Parkinson's disease [8].

The crystal structure of BSA was found to have a heart-like shape at neutral pH condition as determined by x-ray diffraction [9]. This technique gives high resolution of BSA structure at atomic scale as result. However, this method has limitations in the study of protein structure and its conformation especially in solution, because the crystallization of protein can only occur in certain pH and solution condition.

The three-dimensional structure information of BSA in solution with different pH conditions is important to understand the mechanism of protein aggregation-based disease on conformational change of protein. It is also essential to design a perfect protein based-based drug delivery device. Therefore, it is important to study BSA structure in solution by in situ experiment to reveal its structure in several solution conditions.

Small angle neutron scattering (SANS) is considered as a powerful tool to overcome that limitation which can provide low resolution of three-dimensional structural information of macromolecules in solution [10]. Although SANS is a low resolution method, this technique allows to study native protein structures in near physiological conditions and analysis of its structural changes [11]. Here, the structures of BSA in solution were investigated by SANS technique. This study provided conformational structure of BSA in solution which was limited only to structural information, such as the form factor profiles, the shape, and the size.

2.0 METHODOLOGY

Material and Sample Preparation

The BSA powder (A0281) and heavy water D₂O 99.8% (151882) were purchased from the Sigma Chemical Company. All buffer reagents, except acetic acid which was purchased from Sigma, were purchased from Merck (Pro Analysis) and were used without further purification. The BSA solutions were made by dissolving them in D₂O buffer solution. The dissolving process of BSA powder on buffer solution may result in monomeric BSA and small amount of aggregated BSA. Therefore, it was important to make sure that the system was monodisperse containing only monomeric BSA. To obtain that system, the solution was filtered by 100 kDa centrifugal filter. The concentration of 12 mg/ml BSA is measured by UV spectrometer in 280 nm after centrifugation.

Buffer phosphate was applied to obtain the pH of 11, 9 and 7. The pH 7 phosphate buffer was prepared by mixing 0.1 M monosodium phosphate with 0.1 M sodium hydroxide at certain volume. Meanwhile, for pH 9 and 11, the phosphate buffer was prepared by

mixing 0.05 M disodium phosphate with 0.1 M sodium hydroxide at certain volume. The acetate buffer was applied to obtain the pH 5 and 3. The acetic buffer was prepared by mixing 0.1 M acetic acid with 0.1 M sodium acetate at certain volume.

Small Angle Neutron Scattering

The measurements have been performed on the 36 m SANS spectrometer, Neutron Scattering Laboratory BATAN, Indonesia. Each sample was contained in quartz cell with 2 mm inner thickness and exposed to neutron beam with wavelength of 4.9 Å. The measurement was conducted in three configurations of sample-detector distance i.e. 1.3, 4, and 6 m with exposure time for each sample-detector distance was 6, 8 and 8 hours respectively. All measurements were done at ambient temperature. These three configurations were applied to cover the momentum transfer q of 0.02-0.35 Å. The data was subtracted over the background scattering from the buffer solution of each pH condition as well as over the cadmium scattering to correct the data from electronic noise. GRASP data reduction program is applied to do the data reduction [12].

Data Analysis

The size determination by SANS technique is based on the measurement of the elastic neutron scattering intensity as a function of scattering angle, which is transformed as momentum transfer, q ($q=4\pi \sin \theta/\lambda$, where 2θ is scattering angle and λ is neutron wavelength). Assuming the protein as monodisperse system, the scattering intensity is expressed as,

$$I(q) = n(\rho_m - \rho_s)^2 V^2 P(q) S(q) \quad (1)$$

where n denotes the number density of scatterers / particles, ρ_m and ρ_s are the scattering length densities of the protein molecules and the solvent, respectively. The term $(\rho_m - \rho_s)$ is called contrast factor. V is the volume of a protein molecule. $P(q)$ is the intra-particle structure factor and depends on the shape and size of the particles. $S(q)$ is the inter-particle structure factor and is defined by the inter-particle distance and the particle interaction. For dilute solution, $S(q) \sim 1$. The corrected data was then analyzed by Igor NIST data analysis program [13].

In NIST SANS data analysis program, the SANS data of BSA were plotted into log and log one dimensional scattering data and Kratky Plot. The Kratky plot is $I(q) \cdot q^2$ vs q [14] which is useful to check the globularity of the protein.

The initial assumption of BSA shape is approximately closed to triaxial ellipsoidal model. In Igor NIST program, this model calculates the form factor for a triaxial ellipsoid with uniform scattering length density. The function is calculated for an ellipsoid where all three semi-axes are of different

lengths. For the results of the calculation to be valid, the axes are defined as: $R_a \leq R_b \leq R_c$. Th

The chain of contour length, L (the total length) can be described as a chain of some number of locally stiff segments of length l_p . The persistence length, l_p , is the length along the cylinder over which the flexible cylinder can be considered a rigid rod. The Kuhn length (b) used in the model, describes the stiffness of a chain, and is simply define as $b = 2 \cdot l_p$.

For ab initio reconstruction methods, there are several particle parameters that should be computed directly from the experimental data (length and the overall asymmetry). In order to get the information about the overall asymmetry of the scattering particle, the data were further analyzed with ATSAS package program [15]. To determine the maximum dimension, D_{max} , the intra-particle distance distribution function, $p(r)$, was calculated by making use of the GNOM program [16] in which the inverse Fourier transform of $I(q)$ is implemented as follows

$$p(r) = \frac{1}{2\pi^2} \int_0^\infty I(q) \cdot qr \sin(qr) dq \quad (2)$$

This approach provides an alternative method for the calculation of the radius of gyration (R_g) from the full scattering curve. R_g can be expressed by the following equation

$$R_g^2 = \frac{\int r^2 p(r) dr}{2 \int p(r)} \quad (3)$$

The ab initio approaches were employed to reconstruct low-resolution structure models. The program DAMMIF [17] is a development of DAMMIN [18] that run faster. In DAMMIF analysis, the three-dimensional protein model was generated based on pair distribution function. For this study, about 20 raw three-dimensional protein models were generated. These 20 models were then smoothed by stacking and averaging. At the final step, the single three-dimensional protein model was obtained.

3.0 RESULTS AND DISCUSSION

First analysis to reveal the conformational change of BSA was a direct analysis toward SANS spectra of BSA via a Kratky plot (Figure 1). This method can easily determine folded/unfolded state of protein structure. Folded globular proteins typically yield a prominent peak at low angles, whereas unfolded proteins show a continuous increase in $I(q) \cdot q^2$ with q [14]. The peaks presented in this Kratky plot of the BSA at pH 11, 9, 7, and 5, indicating the globular state of this protein. The peak started to disappear in the pH of 3 showed the partially unfolded state in this condition. The peak continuously disappeared, and the intensity began to increase in q in the pH of 2 as the further unfolding of BSA.

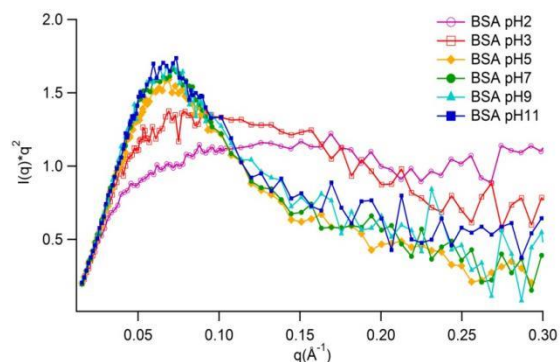
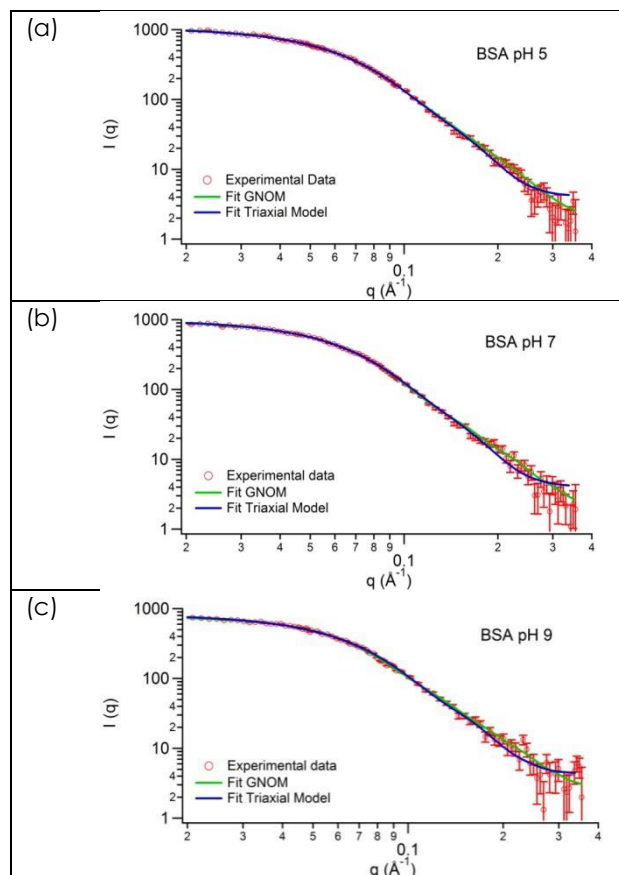


Figure 1 Kratky Plot of BSA as the effect of pH change

SANS data fitting with Igor SANS Analysis shows the globular structure of BSA at pH 11-5. The triaxial ellipsoid model was applied to this system. This model would give simple globular shape with R_a , R_b , and R_c semi-axis in different parameter that can be fitted independently. BSA in pH 5 and 7 (Table 1) have $R_c > R_b > R_a$ values. However, in basic system at pH 9 and 11, the triaxial ellipsoid parameter of R_b increased and followed by decreasing of R_c , resulting in a closed value for those both semi-axes. It means that BSA changed to be more spherical-like in basic solution at pH 9 to 11.



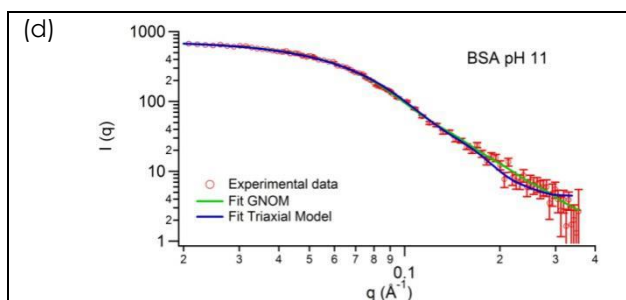


Figure 2 SANS scattering profile of BSA in pH 5, 7, 9 and 11 and the fitting result using simple shape approximation by Igor SANS Analysis and ab-initio calculation by GNOM

Table 1 The fitting result using triaxial ellipsoid model of SANS data analysis

Parameter	BSA pH 5	BSA pH 7	BSA pH 9	BSA pH 11
Ra (Å)	14.3	14.2	14.2	14.5
Rb (Å)	33.6	33.2	37.8	37.3
Rc (Å)	46.7	43.1	38.1	37.4

The fitting result with this model represented the change of two axes but not with one other axis. This shows that the conformation of BSA has changed from N (native) to B (basic) form. The results from simple shape approximation analysis are useful as first assumption to begin an ab-initio calculation with GNOM. Since D_{max} is the maximum distance of the scattering body, the value of R_c were put as initial D_{max} for the calculation in GNOM.

The inter-particle distance distribution function, $p(r)$, of BSA in the range of pH 5-11 (Figure 3) showed a slight change in D_{max} . BSA at pH 5, 7, 9 and 11 have D_{max} of 85 Å, 80 Å, 73 Å and 73 Å respectively. Since $p(r)$ is very sensitive to the overall asymmetry and domain structure of the particle; these data confirm the more globular structure of BSA in alkaline condition. The value of D_{max} of BSA pH 5, 7, 9, and 11 were estimated by trial and error in GNOM with the highest result of 0.894, 0.908, 0.805, and 0.799 respectively which mean good or excellent solution. This calculation generated R_g values of 26.7, 25.7, 24.9 and 24.7 for BSA in pH 5, 7, 9, and 11, respectively. These R_g and D_{max} values confirm that BSA structures are getting little unfold in the more acidic condition of the solution while keeping their globular structure.

Although the fitting curves for these two calculations were slightly different (Figure 2) due to the different calculation formulation and constraint applied in these calculations, the values of R_g obtained from this calculation were similar with the values of R_g obtained by simple shape approximation using Igor SANS Analysis.

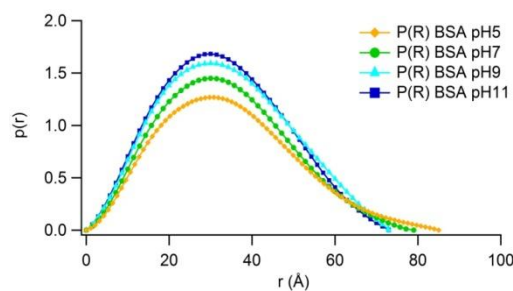


Figure 3 The pair distribution function $p(r)$ of BSA

The result of GNOM was applied to construct the low-resolution structure models using DAMMIF program (Figure 4). The N-form of BSA in pH 7 was compared to the crystal structure of BSA (PDB entry 3V03) [9], illustrated in three orthogonal directions. In this comparison, the BSA model generated from SANS data (in solution) has a good similarity with the crystal structure of BSA.

The low-resolution model of BSA obtained by DAMMIF suggests that the folding of BSA in basic condition was occur in domain II, and make the structure looks shrunk in front view but expanded on side view.

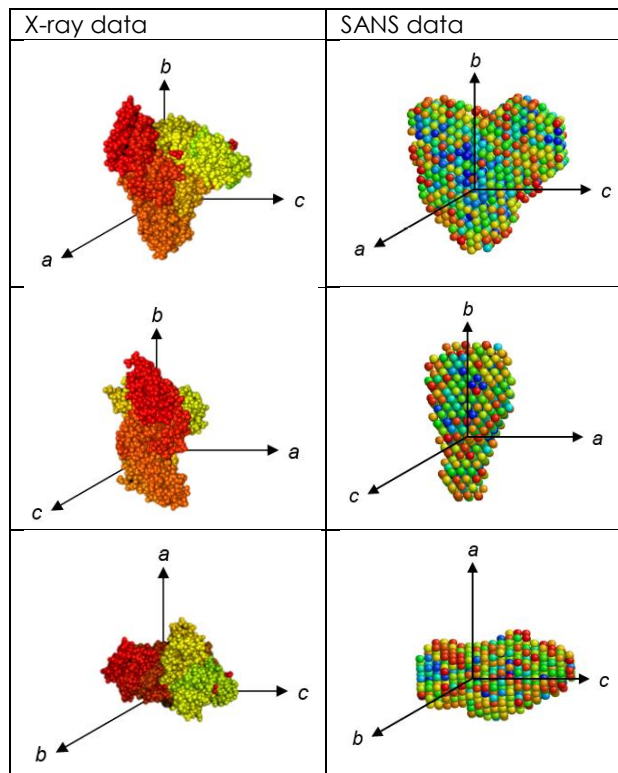


Figure 4 The crystal structure of BSA (PDB entry 3V03), illustrated in three orthogonal directions (left) compared to the low-resolution structure model of N-form BSA, constructed by DAMMIF (right)

The Kratky plot (Figure 1) shows the unchanged peak profile of BSA in pH 5 and 7 (N form) to pH 9 and 11. This indicates that in basic condition, the three-dimensional structure of B and A form of BSA was not different enough from its N form. A report from Ahmad *et al.* suggested that in basic condition BSA has lost its alpha helical content about 3% from its N form structure [19]. However, the loss of secondary structure in B and A form did not alter the tertiary structure of BSA [19]. The fluorescence study shows the stability of the tertiary structure of BSA in pH 9-11. It was also previously reported that the 3% of helical content lost in BSA was occurred in domain I. In domain II, the perturbation of alkaline environment led to rearrangement of domain II with helical twisting. Meanwhile, domain III of BSA was not altered in the alkaline environment [19]. Consequently, the globular structure of BSA in B and A form at pH 9-11 did not change significantly from its N form structure. Another report said that the N-B transition only involved a subtle rearrangement of sub-domain [20,21]. The front view of BSA model (Figure 5), gained from SANS data by DAMMIF program, shows that the heart-like shape of BSA still remained. A slight change in globular structure of BSA in pH 9-11 was observed in the side view of the model indicating the helical twisting occurred in domain II.

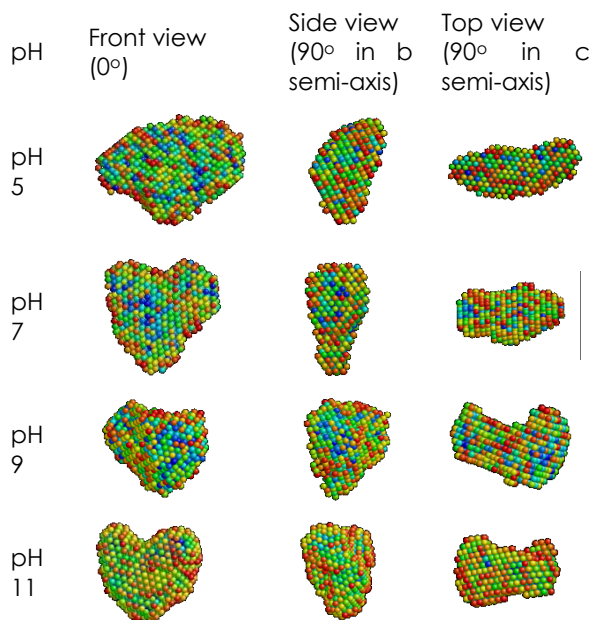


Figure 5 The low-resolution structure model of BSA in pH 5, 7, 9, and 11, constructed by DAMMIF

The Kratky plot (Figure 1), the scattering data analysis (Table 1), and the $p(r)$ function showed that at pH 7 to pH 5, the globular structure of BSA had insignificant expansion. It may be suggested that in this condition, BSA still has negative charge (slightly above its isoelectric point) but not enough basic. The N form of BSA in pH 7 remained in pH 5. Coincident

with the data from DLS study [20], in pH 5, BSA had little expansion.

The N to F (Fast form) transition of BSA was seen in pH 3. The peak of globular BSA, shown in the Kratky plot in Figure 1, decreased and broadened, indicating that the unfolded structure of the protein occurred. Igor SANS analysis shows the unfolding structure of BSA. The simple shape model calculation shows that BSA scattering data in pH 3 fitted with flexible cylinder model (Figure 6) instead of triaxial ellipsoidal one. The radius, Kuhn length, and contour length for BSA in pH 3 were 13, 41 and 162 Å respectively. The calculation of D_{max} at pH 3 gave a value of 100Å, confirming the undergoing of BSA unfolding.

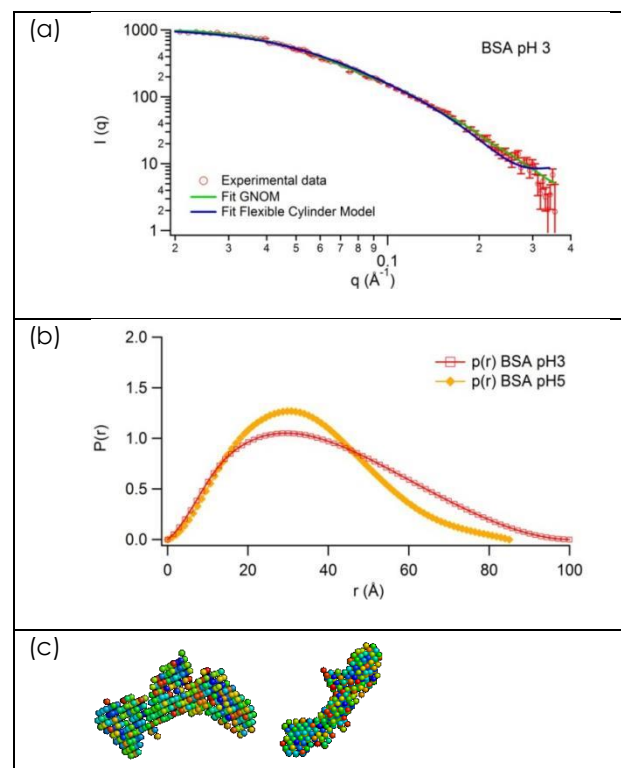


Figure 6 (a) SANS scattering profile of BSA at pH 3, (b) the $p(r)$ function of BSA at pH 3 and 5 show the unfolding process as pH effect and (c) the structural model of F form BSA in pH 3

It has been previously reported that the N-F transition of BSA involved the decreasing of the helical content and localized in the expanding of domain III [20]. However, other study using NMR showed that the expanding of the F state involved not only domain III but a larger part of the protein [19]. The model of BSA at pH 3, constructed by DAMMIF, indicated the possibility of the disruption under acidic condition in the F form involved a larger part and not only in domain III.

At pH values lower than 3, albumin underwent another expansion from F to E transition. The NMR study revealed that the helical content in the transition from F to E form decreased about 9% (from 44 to 35%). In this transition, the separation of BSA domain

increased. This separation created linear bead form due to the disruption of BSA structure in hinge or link region [19]. The expanded form has an increased in the hydrodynamic axial ratio [22] and also increase of about 66% in the length of the protein [20]. The SANS analysis shows the coincident result, in which the result of BSA in pH 2 with Igor SANS Analysis using flexible cylinder model (Figure 7), obtain the value of the radius, Kuhn length and contour length of 10Å, 37Å and 207 Å respectively. However, the three-dimensional model of BSA in pH 2 cannot be constructed by GNOM and DAMMIF due to the loss of rigid body of the BSA itself. In E form, the separation between domains increased. This involved the unfolding of BSA structure from compact structure to linear bead form [19]. It is followed by some loop which became free in some parts of BSA. This made the BSA loose the rigid body and it was difficult to calculate its volume.

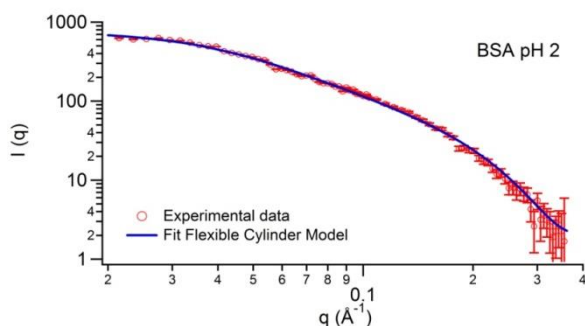


Figure 7 SANS scattering profile of BSA at pH 2

4.0 CONCLUSION

Small angle neutron scattering can provide three-dimensional model structure of globular and unfolded state of BSA in the solution. These results complement the static structure of BSA. It also completed some assumptions about unfolding mechanism of BSA, suggesting that the N-B transition process of BSA involved the subdomain II of BSA and occurred in the pH 7 to pH 9. Meanwhile, the SANS result showed that the transition process of N-F of BSA not only involved subdomain III but also another subdomain of BSA in the pH 5 to pH 3. These three-dimensional structure of BSA at different pH will contribute to the any kind of research involving protein folding-unfolding, such as synthesis of protein-based drug delivery device and protein-based disease study.

Acknowledgement

This work was supported in part by the Academy of Science for the Developing World (TWAS) Research Grant No. 08-140 RG/PHYS/AS, Small-angle Neutron Scattering (SANS) Studies on Biological Macromolecules (PI : Edy Giri R Putra).

References

- [1] Wu, Y., Cheng, H., Chen, Y., Chen, L., Fang, Z., and Liang, L. 2017. Formation of a Multiligand Complex of Bovine Serum Albumin with Retinol, Resveratrol, and (-)-Epigallocatechin-3-gallate for the Protection of Bioactive Components. *J. Agric. Food Chem.* 65: 3019-3030. <http://doi.org/10.1021/acs.jafc.7b00326>.
- [2] Tian, R., Long, X., Yang, Z., Lu, N., and Peng, Y. Y. 2020. Formation of a Bovine Serum Albumin Dligand Complex with Rutin and Single-walled Carbon Nanotubes for the Reduction of Cytotoxicity. *Biophys. Chem.* 256: 106268. <http://doi.org/10.1016/j.bpc.2019.106268>.
- [3] Zhang, Y., Sun, T., and Jiang, C. 2018. Biomacromolecules as Carriers in Drug Delivery and Tissue Engineering. *Acta Pharm. Sin. B.* 8: 34-50. <http://dx.doi.org/10.1016/j.apsb.2017.11.005>.
- [4] Gharbavi, M., Manjili, H.K., Amani, J., Sharafi, A., and Danafar, H. 2019. In Vivo and In Vitro Biocompatibility Study of Novel Microemulsion Hybridized with Bovine Serum Albumin as Nanocarrier for Drug Delivery. *Heliyon*. 5: e01858. <http://doi.org/10.1016/j.heliyon.2019.e01858>.
- [5] Afridi, M. N., Lee, W. H., and Kim, J. O. 2020. Application of Synthesized Bovine Serum Albumin-Magnetic Iron Oxide for Phosphate Recovery. *J. Ind. Eng. Chem.* 86: 113-122. <http://doi.org/10.1016/j.jiec.2020.02.018>.
- [6] Foster, J. F. 1977. *Some Aspects of the Structure and Conformational Properties of Serum Albumin*. Pergamon Press Inc. <http://dx.doi.org/10.1016/B978-0-08-019603-9.50010-7>.
- [7] Raskin, J., Cummings, J., Hardy, J., Schuh, K., and Dean, R. 2015. Neurobiology of Alzheimer's Disease: Integrated Molecular, Physiological, Anatomical, Biomarker, and Cognitive Dimensions. *Curr. Alzheimer Res.* 12: 712-722. <http://doi.org/10.2174/1567205012666150701103107>.
- [8] Olanow, C. W., and Tatton, W. G. 1999. Etiology and Pathogenesis of Parkinson Disease. *Neurol. Clin.* 22: 123-144. <http://doi.org/10.1016/j.ncl.2009.04.004>.
- [9] Majorek, K. A., Porebski, P. J., Dayal, A., Zimmerman, M. D., Jablonska, K., Stewart, A. J., Chruszcz, M., and Minor, W. 2012. Structural and immunologic Characterization of Bovine, Horse, and Rabbit Serum Albumins. *Mol. Immunol.* 52: 174-182. <http://doi.org/10.1016/j.molimm.2012.05.011.Structural>.
- [10] Jacques, D. a., and Trehwella, J. 2010. Small-angle Scattering for Structural Biology - Expanding the Frontier while Avoiding the Pitfalls. *Protein Sci.* 19: 642-657. <http://doi.org/10.1002/pro.351>.
- [11] Patriati, A., Suparno, N., Sulungbudi, G. T., Mujamilah, M., and Putra, E. G. R. 2020. Structural Change of Apoferitin as the Effect of pH Change: Dls and Sans Study. *Indones. J. Chem.* 20.
- [12] Dewhurst, C. 2003. GRASP User Manual. *Tech. Rep. No. ILL03DE01T*. <http://www.ill.fr/lss/grasp>.
- [13] Kline, S. R. 2006. Reduction and Analysis of SANS and USANS Data using IGOR Pro. *J. Appl. Crystallogr.* 39: 895-900. <http://doi.org/10.1107/S0021889806035059>.
- [14] Doniach, S. 2001. Changes in Biomolecular Conformation Seen by Small Angle X-ray Scattering. *Chem. Rev.* 101: 1763-1778. <http://10.0.3.253/cr990071k>.
- [15] Petoukhov, M. V., Franke, D., Shkumatov, A. V., Tria, G., Kikhney, A.G., Gajda, M., Gorba, C., Mertens, H. D. T., Konarev, P. V., and Svergun, D. I. 2012. New Developments in the ATSAS Program Package for Small-angle Scattering Data Analysis. *J. Appl. Crystallogr.* 45: 342-350. <http://doi.org/10.1107/S0021889812007662>.
- [16] Svergun, D. I., Petoukhov, M. V., and Koch, M. H. 2001. Determination of Domain Structure of Proteins from X-ray Solution Scattering. *Biophys. J.* 80: 2946-2953. [http://dx.doi.org/10.1016/S0006-3495\(01\)76260-1](http://dx.doi.org/10.1016/S0006-3495(01)76260-1).
- [17] Franke, D., and Svergun, D. I. 2009. DAMMIF, A Program for Rapid ab-initio Shape Determination in Small-angle

- Scattering. *J. Appl. Crystallogr.* 42: 342-346. <http://doi.org/10.1107/S0021889809000338>.
- [18] Svergun, D. I. 1999. Restoring Low Resolution Structure of Biological Macromolecules from Solution Scattering Using Simulated Annealing. *Biophys. J.* 76: 2879-86. [http://doi.org/10.1016/S0006-3495\(99\)77443-6](http://doi.org/10.1016/S0006-3495(99)77443-6).
- [19] Ahmad, B., Kamal, M. Z., and Khan, R. H. 2004. Alkali-induced Conformational Transition in Different Domains of Bovine Serum Albumin. *Protein Pept. Lett.* 11: 307-315. <http://doi.org/10.2174/0929866043406887>.
- [20] Sadler, P. J., and Tucker, A. 1993. pH-induced Structural Transitions of Bovine Serum Albumin. Histidine Pka Values and Unfolding of the N-Terminus during the N to F transition. *Eur. J. Biochem.* 212: 811-7. <http://doi.org/10.1111/j.1432-1033.1993.tb17722.x>.
- [21] Kun, R., Szekeres, M., and Dekany, I. 2009. Isothermal titration Calorimetric Studies of the Ph Induced Conformational Changes of Bovine Serum Albumin. *J. Therm. Anal. Calorim.* 96: 1009-1017. <http://doi.org/10.1007/s10973-009-0040-5>.
- [22] Harrington, W. F., Johnson, P., and Ottewill, R. H. 1954. Bovine Serum Albumin and its Behaviour in Acid Solution. *Biochem. J.* 62: 569-582. <https://doi.org/10.1042/bj0620569>.